Recombination processes and photoluminescence intensity in quantum wells under steady-state and transient conditions

O. Brandt,* K. Kanamoto, M. Gotoda, T. Isu, and N. Tsukada
Semiconductor Research Laboratory, Mitsubishi Electric Corporation, 1-1, Tsukaguchi-honmachi 8-chome, Amagasaki, Hyogo 661, Japan
(Received 21 March 1994; revised manuscript received 29 November 1994)

We present a theoretical and experimental study of recombination processes in quantum wells. Our model calculations, which include free-excitonic, free-carrier, and defect-mediated nonradiative recombination, describe the dependence of the photoluminescence intensity on excitation density under steady-state conditions and on time under transient conditions. For the former conditions, it is not, in principle, possible to distinguish between excitonic and free-carrier contributions to the photoluminescence intensity. However, an accurate determination of the relative weight of nonradiative and radiative contributions can be made. For transient conditions, on the other hand, excitonic contributions may be identified, while the discrimination between radiative and nonradiative contributions is—though possible—possessed with ambiguities. We finally apply our model to a set of experimental data, taken at 300 K from a single $In_{0.1}Ga_{0.9}As/Al_{0.33}Ga_{0.67}As$ quantum well under both steady-state and transient conditions. The results of this analysis demonstrate the consistency of our model and its potential for the quantitative understanding of the recombination dynamics in quantum wells.

I. INTRODUCTION

Recombination processes in semiconductors have been the subject of worldwide theoretical and experimental research for several decades.[1] From the very beginning, these efforts have been vitally motivated by the importance of a quantitative understanding of recombination processes for the design of optoelectric devices, such as lasers and photodetectors. However, this understanding is, at present, far from complete, particularly so in the case of quantum wells, for which the nature of the dominant recombination channels at certain experimental conditions is still highly controversial.[2] The main reason for this unsatisfactory situation is the great variety of recombination channels which make a general theoretical description difficult, and an unambiguous interpretation of experiments almost impossible.[3] Even if we restrict ourselves to the case of relatively low excitation densities, where Auger recombination may be neglected, and comparatively high temperature, where impurity and bound-exciton recombination become unimportant,[4] there still remain two recombination channels in addition to free-carrier recombination which seem to be important in the case of quantum wells. First, it has been argued that, in contrast to bulk crystals, free-excitonic recombination contributes to the emission of quantum wells (QW's) even at room temperature (RT) because of their enhanced binding energy with respect to the bulk.[5] In fact, this presumption is convincingly illustrated by the appearance of distinct excitonic peaks in photoluminescence (PL) spectra recorded at 300 K,[6] and by the coincidence of these peaks with exciton resonances in absorption-related spectra.[7] Second, it has been suggested that nonradiative interface recombination becomes the dominant recombination channel in quantum wells because of the close vicinity of interfaces corresponding to an effective high density of recombination centers.[2] In fact, the overwhelming majority of values for the RT nonradiative lifetimes reported in the literature are on the order of nanoseconds, and thus orders of magnitude shorter than small-signal radiative lifetimes for undoped quantum wells.[8]

It is clear from the above that a comprehensive model for recombination processes in QW's has, in general, to treat free-carrier, free-exciton, and nonradiative recombination on equal footing. Such a model, however, has not yet been developed to our knowledge. It is the purpose of the present paper to fill this gap. The most complete models of recombination processes in quantum wells to date have been developed independently by Pickin and David[2] and by Ridley.[9] Both these models are, at first, identical, in that they are based on the standard coupled rate-equation approach for describing the recombination dynamics under transient conditions (PL decay).[1] The two approaches, however, differ in their simplifying assumptions. Pickin and David conclude, on the basis of order-of-magnitude estimations, that the PL decay is governed by interface recombination, whereas excitons may be safely neglected at RT. In contrast, Ridley emphasizes the importance of excitonic recombination even at RT, but neglects defect-mediated nonradiative recombination on the basis of an optimistic estimation of the present material quality.

Here we follow the same basic approach as our predecessors but do not, at any stage, neglect excitonic or nonradiative recombination. We solve the basic rate equations for steady-state and transient conditions and calculate the corresponding PL intensity as a function of excitation density and of time, respectively. We discuss the influence of excitonic contributions, doping, and trap

0163-1829/95/51(11)/7029(9)/$06.00 ©1995 The American Physical Society

density on the photoluminescence intensity with particular emphasis on situations of practical relevance. Conditions to be fulfilled for a reliable interpretation of experimental data are pointed out. The analysis of a particular set of experiments demonstrates the ability of our model for the unique determination of the small-signal radiative and nonradiative lifetimes.

II. THEORY

A. Basic rate equations

We begin our analysis with the recapitulation of the basic rate equations describing the carrier dynamics in a quantum well. As indicated above, we restrict ourselves to the case of temperatures high enough for radiative recombination involving localized excitons and impurities to be neglected, and of carrier densities low enough such that Auger recombination is not important. For GaAs-based quantum wells, these assumptions are valid for temperatures above 30 K and carrier densities below 10^{13} cm^{-2}. Furthermore, exciton screening (which will be important for carrier densities above about 2×10^{11} cm^{-2}) is only considered qualitatively because its explicit treatment makes the model mathematically rather difficult to handle. Finally, we concentrate on single quantum wells (SQW's) for which we can safely neglect nonuniform excitation conditions and photon recycling. In general, both of these phenomena must be considered for multiple quantum wells.[3,9]

Given these considerations, we can now formulate the equations describing the carrier dynamics in a SQW upon carrier injection with the rate G as

$$\frac{dn}{dt}=G-b_r(np-n_0p_0)-b_nn_t^+n-f_xnp+d_xn_x\ , \quad (1)$$

$$\frac{dp}{dt}=G-b_r(np-n_0p_0)-b_pn_t^0p-f_xnp+d_xn_x\ , \quad (2)$$

$$\frac{dn_x}{dt}=-\gamma_x(n_x-n_{x0})+f_xnp-d_xn_x\ , \quad (3)$$

where n, p, and n_x are the electron, hole, and exciton densities, n_0, p_0 and n_{x0} are their respective equilibrium values, b_r is the radiative band-to-band recombination coefficient, γ_x is the radiative decay rate of excitons, b_n and b_p are the nonradiative recombination coefficients for electron and holes,[10] n_t^+ and n_t^0 are the densities of empty and filled recombination centers, and d_x and f_x are the rate coefficients for the dissociation and formation of excitons. The latter terms are particularly important at higher temperatures, where the population of optical phonons becomes significant.

In order to simplify the coupled rate-equation system (1)–(3), we presume, as is commonly done, that both electron and hole capture by the recombination centers[11] and the dissociation and formation of excitons[2,9] establish (independent) quasiequilibria between the respective particle populations. Detailed balance then implies (i) $b_nn_t^+n\approx b_pn_t^0p$ and (ii) $f_xnp\approx d_xn_x$. These relations are, strictly speaking, only valid for higher temperatures, for which the participating processes are rapid compared to radiative recombination. For low temperature these approximations are bound to fail, but the corresponding terms are then small enough to be neglected altogether, which decouples the rate-equation system (1)–(3). The first of the detailed balance conditions allows the elimination of Eq. (2). The substitution of the second condition into the sum of Eqs. (1) and (3) eliminates n_x. Finally, we consider p-type background doping for which $np-n_0p_0=\Delta n(p_0+\Delta n)$ with the photogenerated excess carrier density Δn. (In the following, we will refer to recombination processes which originate from the terms linear and quadratic in Δn as monomolecular and bimolecular, respectively.) The resulting equation can be written as

$$\frac{d}{dt}[\Delta n(1+\sigma_xp_0+\sigma_x\Delta n)]=G-B\Delta n(p_0+\hat{N}_t+\Delta n)\ , \quad (4)$$

where we have introduced the exciton cross section $\sigma_x=f_x/d_x$, the effective radiative recombination coefficient $B=b_r+b_x$ including the contributions of free carriers and excitons ($b_x=\sigma_x\gamma_x$), and the effective density of recombination centers $\hat{N}_t=(b_{nr}/B)N_t$, i.e., the total density of recombination centers $N_t=n_t^++n_t^0$ weighed with the ratio of the nonradiative and radiative recombination coefficients. Equation (4), which forms the basis of our model, includes the models of Pickin and David[2] and of Ridley,[9] and reduces to them in the limit of $\sigma_x\to0$ and $\hat{N}_t\to0$, respectively.

Prior to the discussion of Eq. (4) for both steady-state and transient conditions in the following paragraphs, we comment on two of the quantities defined above, namely (i) the nonradiative lifetime $(b_{nr}N_t)^{-1}$ and (ii) the exciton cross section σ_x.

(i) The above considered quasiequilibrium between empty and filled recombination centers leads to the familiar Shockley-Read-Hall (SRH) expression for the nonradiative rate.[11,12] The common definition of a single nonradiative lifetime independent of carrier density is thus an approximation whose validity is not clear *a priori,* as the values of b_n and b_p for a specific recombination center responsible for the nonradiative process are, in general, unknown. It is, however, often realistic to assume that the capture coefficient for minority carriers is much larger than that for majority carriers, and, consequently, that center saturation and thus the linear regime is already established at modest excitation levels.[11] For the sake of simplicity, we therefore follow the common practice and write the nonradiative term as $b_{nr}N_t\Delta n$ with an unspecified constant nonradiative recombination coefficient b_{nr}.

(ii) The exciton cross section σ_x introduced in Eq. (4) is, at thermal equilibrium, equal to n_{x0}/n_0p_0 and is thus readily obtained from exciton and free-carrier statistics[1] as

$$\sigma_x=\frac{2}{N_{cv}}e^{E_x/kT}\int_0^{E_x/kT}\sqrt{\eta}e^{-\eta}d\eta\ , \quad (5)$$

with the reduced density of states $N_{cv}=\mu kT/\pi\hbar^2$, where μ is the reduced mass of the exciton, and $\eta=E/kT$ with

the exciton's kinetic energy E. The upper limit of integration E_x/kT takes care of the fact that the number of excitons is not conserved, i.e., excitons with kinetic energy exceeding their binding energy are likely to be dissociated into free carriers.[1,13] This condition guarantees $\sigma_x \to 0$ for $E_x/kT \to 0$. Furthermore, we see that σ_x monotonically increases with the exciton binding energy E_x, i.e., σ_x can be understood as the cross section for the scattering of free carriers into the exciton state. Alternatively, we may also conclude that σ_x phenomenologically describes the effect of inelastic optical-phonon scattering on the exciton lifetime. As will be shown in Sec. II C, the low-temperature exciton lifetime $(\gamma_x)^{-1}$ is modified at higher temperatures and eventually approaches $(\gamma_x \sigma_x p_0)^{-1}$. This high-temperature lifetime increases roughly exponentially with kT, in contrast to the linear dependence at low temperatures caused by quasielastic scattering with acoustic phonons.

B. Steady-state solution

For steady-state conditions, Eq. (4) is equal to zero, and the generation term G is constant. The PL intensity (defined as the sum of the monomolecular and bimolecular terms) as a function of the generation rate is then given by

$$I_{\mathrm{PL}}(G) = \frac{G^*}{1+\tau_{\mathrm{nr}}/\tau_r}\left[1+\left[1+\frac{\tau_{\mathrm{nr}}}{\tau_r}\right]\frac{G}{G^*} - \left[1+2\frac{G}{G^*}\right]^{1/2}\right], \tag{6}$$

with the constant $G^* = (2B\tau^2)^{-1}$, where we have defined the effective lifetime τ as $1/\tau = 1/\tau_r + 1/\tau_{\mathrm{nr}} = B(p_0 + \hat{N}_y)$. For $G \ll G^*$, Eq. (6) reduces to $I_{\mathrm{PL}} \sim \eta G$, where $\eta = (1+\tau_r/\tau_{\mathrm{nr}})^{-1}$ is the small-signal quantum efficiency. In this regime, the PL intensity is limited by the competition between the monomolecular radiative and nonradiative process. In the case of $G \gg G^*$ we obtain $I_{\mathrm{PL}} \sim G$; i.e., in the large-signal (bimolecular) regime we ultimately approach the intrinsic limit. In both cases, however, the PL intensity depends linearly on G. A deviation from linearity is only expected in the transition regime between these two extremes, and is caused by the simultaneous occurrence of bimolecular radiative and nonradiative recombinations of comparable magnitude. The takeover of the bimolecular term ($\sqrt{GB}$) with respect to the combined monomolecular radiative and the nonradiative terms $(1/\tau)$ is characterized by the condition $G/G^* \approx 1$. We emphasize that a correct interpretation of experimental data using Eq. (6) requires direct excitation of the QW. If the QW is excited indirectly (i.e., by carrier capture from the directly excited barrier material), G represents the carrier capture term which itself exhibits a complex dependence on the actual generation rate.

An equation formally identical to Eq. (6) has been derived previously by Böttcher *et al.*[14] However, these authors erroneously interpreted the radiative lifetime τ_r as originating solely from excitons. In fact τ_r, while including the excitonic contribution, principally stems from the monomolecular term of free-carrier recombination. More recently, Ding *et al.*[15] analyzed their experimental PL intensity data on the basis of a model similar to ours, neglecting, however, the monomolecular term which is equivalent to setting $\tau_{\mathrm{nr}}/\tau_r = 0$ in Eq. (6).

Since experimental values for the band-to-band recombination coefficient are highly controversial,[16] and do not exist for the excitonic recombination coefficient, we derive values for b_r and b_x theoretically (see Sec. II C). The free parameters remaining in our model are the dark hole density p_0 and the nonradiative lifetime τ_{nr}. For a close connection with experiments, in the following discussion we use the laser intensity rather than the generation rate, which are related by $G = p\phi$, where p is the absorption probability per layer[17] and ϕ is the photon flux given by the laser intensity per photon energy.

Figure 1 shows selected examples of the steady-state PL intensity as a function of the laser intensity calculated for a fixed nonradiative lifetime of 10 ns for various values of the small-signal radiative lifetime. The upper dashed line represents the intrinsic limit $I_{\mathrm{PL}} = G$. As we see, a longer small-signal radiative lifetime (equivalent to a decreasing background doping level) leads to an increasingly pronounced superlinear behavior for intermediate and small laser intensities. Ultimately, a purely quadratic dependence on laser intensity is obtained, corresponding to the experimental data of Ding *et al.*[15] For high laser intensities, all curves ultimately approach the intrinsic limit and thus follow its linear dependence on laser intensity. This transition occurs, naturally, at smaller laser intensities for smaller nonradiative contributions. The curves also evidence the importance of a large dynamic range in actual measurements, i.e., the PL intensity should be recorded over several decades of laser intensity. The dynamic range of three decades used for the simulations depicted in Fig. 1 is experimentally realistic and usually sufficient for the identification of the participating recombination channels.

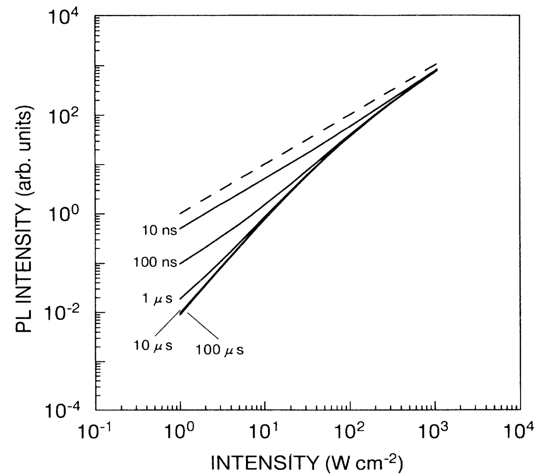

FIG. 1. Steady-state PL intensity as a function of laser intensity for a constant nonradiative lifetime of 10 ns and various values for the radiative lifetime as denoted in the figure. The dashed uppermost line represents the intrinsic limit $I_{\mathrm{PL}} = G$.

We stress that, experimentally, the absolute value of the PL intensity is very difficult to determine. Experimental PL intensity data which are largely parallel to each other are, consequently, hardly distinguishable. To evaluate the potential precision of such measurements in determining the radiative and nonradiative lifetimes, we examine the laser-intensity dependence of the PL intensity upon changes of the radiative and nonradiative lifetimes within a factor of 2. For doing so, it is advantageous to plot the derivative of the PL intensity with respect to laser intensity (the PL efficiency profile), as shown in Fig. 2 for two sets of neighboring values for the radiative and nonradiative lifetimes. Each of the profiles of a given set can indeed be distinguished from the other. Least-squares fits to these simulated profiles gave radiative and nonradiative lifetimes essentially identical to the input parameters of the simulations. However, some of the profiles are actually almost parallel to each other (see, for example, the two profiles with a radiative lifetime of 1 μs), and the inevitable noise of actual experimental data may wash out the subtle differences present in the theoretical curves. We thus regard a precision within a factor of 2 as a realistic estimate for the precision obtainable in experimental situations.

C. Transient solution

Next we consider the transient solution of Eq. (4). In this case, G can be approximated by a δ function, and the decay of the excess carrier density Δn after excitation is determined by

$$\Delta n \left[\frac{\Delta n + p_0 + \hat{N}_t}{\Delta n_0 + p_0 + \hat{N}_t} \right]^y = \Delta n_0 e^{-t/\tilde{\tau}} , \tag{7}$$

where Δn_0 is the excess carrier density at $t=0$. The exponent y is given by

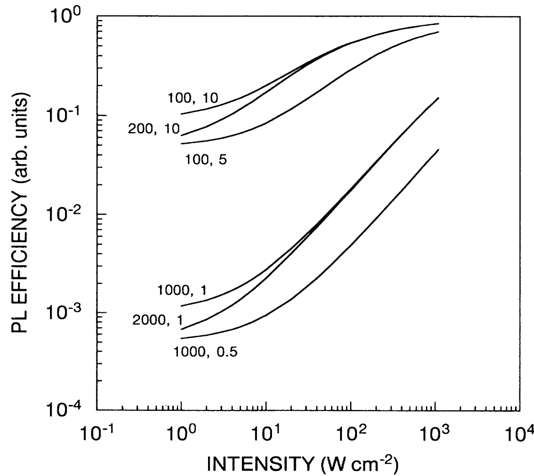

FIG. 2. Derivative of the steady-state PL intensity with respect to laser intensity for two sets of neighboring values for the radiative and nonradiative lifetimes ($\tau_r, \tau_{\mathrm{nr}}$) in ns as denoted in the figure.

$$y = \frac{\sigma_x (p_0 + 2\hat{N}_t) - 1}{1 + \sigma_x p_0} , \tag{8}$$

and may lie, mathematically, within the range $-1 \leq y < \infty$. For physically realistic parameters, y will range between -1 and 2. The effective decay time $\tilde{\tau}$ is given by

$$\frac{1}{\tilde{\tau}} = \frac{B(p_0 + \hat{N}_t)}{1 + \sigma_x p_0} . \tag{9}$$

Note that $\tilde{\tau}$ differs from the effective lifetime τ for steady-state conditions due to the excitonic correction $\sigma_x p_0$.

Equation (7) is an implicit equation in $\Delta n(t)$ which cannot, for general values of y, be solved in closed analytical form. It is even difficult to find sensible approximations which are valid for arbitrary y, particularly so for the large-signal limit. In this respect, it is quite instructive to examine Eq. (7) with respect to special values of y, and to discuss the temporal behavior of these special solutions.

We first consider the case $y=-1$ which is obtained for $\sigma_x = 0$ corresponding to pure free-carrier recombination (including radiative and nonradiative contributions). We can then solve Eq. (7) analytically and calculate the PL intensity as a function of time as

$$I_{\mathrm{PL}}(t) = \frac{\frac{\Delta n_0}{\tau_r}(1+\alpha) e^{-t/\tau} + \frac{\Delta n_0}{\tau_{\mathrm{nr}}} \alpha e^{-2t/\tau}}{[1 + \alpha(1 - e^{-t/\tau})]^2} , \tag{10}$$

where we defined the dimensionless effective injection level $\alpha = \Delta n_0 / (p_0 + \hat{N}_t)$. For the large-signal case ($\alpha \gg 1$) we can approximate the initial decay ($t \ll \tau$) as

$$I_{\mathrm{PL}}(t) = \frac{b_r \Delta n_0^2}{(1 + b_r \Delta n_0 t)^2} , \tag{11}$$

which represents the well-known hyperbolic decay for pure bimolecular recombination.[18] For the small-signal case ($\alpha \ll 1$), on the other hand, we obtain the single-exponential decay characteristic for monomolecular recombination:

$$I_{\mathrm{PL}}(t) = b_r p_0 \Delta n_0 e^{-t/\tau} . \tag{12}$$

The PL decay in the small-signal regime is thus governed by the effective lifetime τ, which reflects the competition between the monomolecular radiative and nonradiative channels. Note that the distinction between radiative and nonradiative contributions to the effective lifetime is, without further independent information, not free of ambiguities. In this respect, the analysis of the steady-state PL intensity, as outlined in Sec. II B, provides a valuable aid for the correct interpretation of transient measurements.

Next we consider the case $\sigma_x p_0 \to \infty$, which leads to $y=1$ representing pure excitonic recombination (neglecting nonradiative contributions). We find that the PL intensity can be written, regardless the excitation level, as

$$I_{\mathrm{PL}}(t) = b_x \Delta n_0 (p_0 + \Delta n_0) e^{-\gamma_x t} . \tag{13}$$

Pure excitonic recombination is, in fact, the only case where a single-exponential decay is predicted for any excitation level, as stated previously by Ridley.[9]

An examination of Eqs. (11) and (13) indicates that the relative magnitudes of the radiative recombination coefficients for free carriers and excitons may strongly affect the decay behavior. For realistic simulations of the PL decay as well as for a reliable interpretation of experimental data, we thus need explicit values for both recombination coefficients. The band-to-band recombination coefficient b_r for a QW is readily obtained from standard perturbative treatments of spontaneous emission processes.[19] For determining the exciton recombination coefficient b_x we employ the formalism developed by Andreani, Tassone, and Bassani[20] and more recently by Citrin,[21] which properly takes into account that only excitons with a kinetic energy lower than E_1 (below the crossing with the photon line) are allowed to undergo radiative decay. We note that the resulting expression for the radiative decay rate of the exciton is different from that used by Ridley and Bishop[3,9] which was shown by Citrin[21] to be valid only for very low temperatures (<1 K) and otherwise to significantly overestimate the decay rate.

As a numerical example, we obtain $b_r = 7.2\times10^{-4}$ cm^2/s and $b_x = 4.8\times10^{-4}$ cm^2/s at 300 K for a 5-nm-thick GaAs QW (Ref. 22) with an exciton binding energy of $E_x = 12$ meV. As we see, band-to-band and exciton recombination coefficients are predicted to be of the same order of magnitude even at 300 K. Because these coefficients are a measure of the PL intensity, the observation of excitonic peaks in RT-PL spectra of narrow QW's becomes quite plausible.

Figure 3 shows the simulated PL decays at 77 K calculated by means of Eq. (7) for a nonradiative contribution with $\tau_{nr} = 20$ ns. We compare the decay which arises when excitons are neglected ($\sigma_x = 0$, $b_x = 0$, and $b_r = 2.84\times10^{-3}$ cm^2/s) to that when they are properly taken into account ($\sigma_x = 6.3\times10^{-11}$ cm^2, $b_x = 1\times10^{-1}$ cm^2/s, and b_r as above), assuming a background hole density of $p_0 = 5\times10^8$ cm^{-2} and an initial excess carrier density of $\Delta n_0 = 5\times10^{11}$ cm^{-2}. It is clear that the inclusion of excitons at 77 K is crucial, as their presence substantially modifies the decay behavior. In particular, the initial decay in fact becomes exponential if excitons are included, whereas the pure free-carrier decay follows the expected hyperbolic behavior. We note, however, that the initial excess carrier concentration assumed for the calculation is already in a regime where exciton screening is important. Taking exciton screening into account, we expect the actual decay to be close to the lower envelope of the two decay curves. The behavior of the two decay curves at long times is practically identical because of the presence of the nonradiative channel which completely dominates the small-signal regime.

Figure 4 shows the simulated PL decays at 300 K calculated by means of Eq. (7), again for a nonradiative contribution with $\tau_{nr} = 20$ ns. As above, we compare the decay for the pure free-carrier case ($\sigma_x = 0$, $b_x = 0$, and $b_r = 7.2\times10^{-4}$ cm^2/s) to that when excitons are included ($\sigma_x = 1.1\times10^{-12}$ cm^2, $b_x = 4.8\times10^{-4}$ cm^2/s, and b_r as above) for the same values for p_0 and Δn_0 as before. Although the complete (free carrier and excitonic) decay is still distinguishable from that of free carriers alone, the differences are quite subtle. Taking into account the fact that exciton screening will bring the complete decay even closer to that of free carriers alone, we are thus led to the conclusion that the RT-PL decay of intentionally undoped GaAs QW's, i.e., with typical doping levels of $10^8 \ldots 10^9$ cm^{-2}, is only insignificantly influenced by excitonic recombination. However, for lightly doped GaAs QW's [$p_0 \sim (3\ldots6)\times10^{10}$ cm^{-2}, i.e., well below the occurrence of complete exciton screening] the quantity

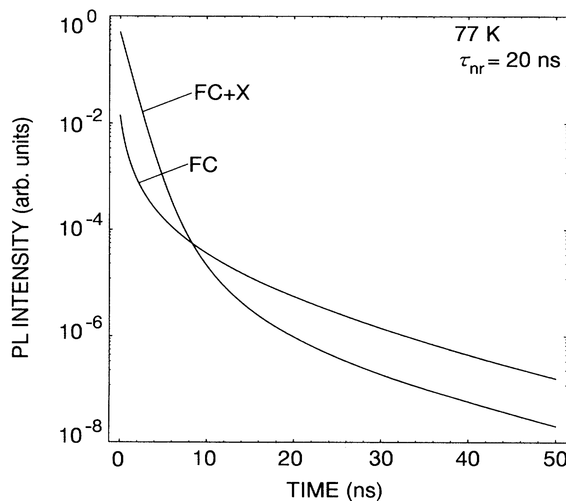

FIG. 3. Transient PL intensity at 77 K for a nonradiative contribution of $\tau_{nr} = 20$ ns. The decay of free carriers alone (FC) is compared to that of free carriers and excitons together (FC+X).

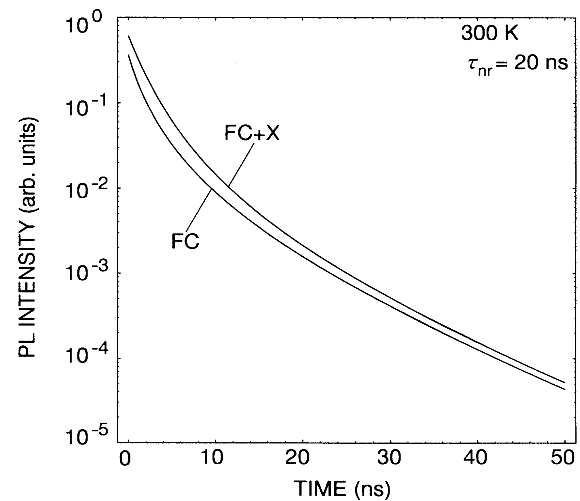

FIG. 4. Transient PL intensity at 300 K for a nonradiative contribution of $\tau_{nr} = 20$ ns. The decay of free carriers alone (FC) is compared to that of free carriers and excitons together (FC+X).

$\sigma_x p_0$ becomes comparable to that obtained above at 77 K even at RT, and excitonic effects consequently must not be neglected. The argument of Pickin and David[2] that, at RT, one may neglect excitons at any carrier density which permits them to exist, is thus not correct in general. Furthermore, in material systems such as wide-gap II-VI compounds, which are characterized by a significantly larger (4×) exciton binding energy than III-V compounds, the RT PL is certainly affected and may even be dominated by the radiative decay of excitons.

Finally, it is seen from Figs. 3 and 4 that, similar to the case of steady-state excitation, a large dynamic range is essential for an unambiguous interpretation of an experimental PL decay. However, the commonly achievable dynamic range of three or, at most, four orders of magnitude in a single measurement is in general not sufficient for deducing the correct shape of the PL decay (see, e.g., Fig. 3). The combination of measurements with decreasing initial excitation level and increasing detection sensitivity may thus be necessary to reveal, for example, deviations from an apparently single-exponential decay.

III. EXPERIMENT

In this section, we analyze steady-state and transient PL data obtained on a single $In_{0.1}Ga_{0.9}As/Al_{0.33}Ga_{0.67}As$ QW by means of the model developed in Sec. II. The sample under consideration was grown by solid-source molecular-beam epitaxy (MBE) on an exactly (311) *A*-oriented ($<0.05°$ off) Si-doped GaAs substrate and using an As cracker cell providing As_2 dimers as the As source. The layer sequence consists of 200 nm of GaAs, a 100-period GaAs/AlAs superlattice buffer with an individual layer thickness of 4 nm, and a nominally 5-nm-thick $In_{0.1}Ga_{0.9}As$ QW clad by 300-nm-thick $Al_{0.33}Ga_{0.67}As$ barrier layers. The whole structure is intentionally undoped.

Photoluminescence and photoluminescence excitation spectra taken at 4 K attest to the high optical quality of this sample, as demonstrated (i) by the narrow linewidth of the heavy-hole exciton resonance of 2.5 meV, which is among the best values ever reported for $In_xGa_{1-x}As/Al_yGa_{1-y}As$ QW's ($y>0$),[23] and (ii) by the appearance of the exciton continuum edge in the excitation spectrum. The latter observation allows us directly to deduce the exciton binding energy of the present sample, which was thus measured to be 12 meV. PL spectra taken at RT exhibit clear excitonic resonances at the spectral position of the heavy and light-hole exciton states, similar to the above-mentioned reports.[6]

A. Steady-state conditions

Steady-state PL measurements are performed at 300 K using an Ar^+-ion laser-pumped Ti-sapphire laser set to a wavelength of 768 nm as the excitation source. The laser power is adjusted by means of neutral density filters and carefully measured with a Newport 835 high-precision digital powermeter. The $1/e^2$ diameter of the laser spot focused onto the sample surface is determined by a pinhole moved through the beam. Finally, the laser intensity on the sample is calculated assuming Gaussian optics, including corrections for reflection losses. The emitted light is dispersed by a 0.75-m monochromator and detected by a GaAs photomultiplier connected to a lock-in amplifier. The PL intensity was obtained by numerical integration over the whole PL spectrum.

In Figs. 5(a) and 5(b), we show the experimental data and their best fit [Eq. (6)] of the PL intensity as a function of laser intensity (a) and the corresponding PL efficiency profile (b) for the sample under consideration. For the original data (a) the size of the data points is adjusted to represent the actual experimental uncertainty. The fit of Eq. (6) to these data is superb. Close examination reveals that the data do not follow a straight line, but exhibit a behavior similar to that of the simulated curve for $\tau_r=100$ ns in Fig. 1, namely a linear dependence for small and large laser intensities joined by a slightly superlinear region at intermediate intensities. This behavior is more evident in Fig. 5(b), where, indeed, the derivative of the PL intensity is seen to be constant for small and high

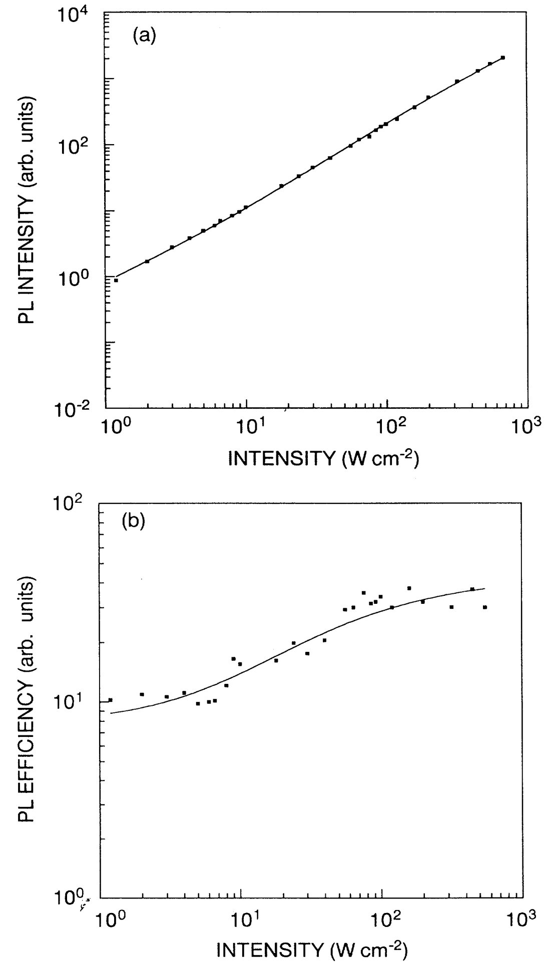

FIG. 5. Steady-state PL intensity as a function of laser intensity (a) and its derivative (b) of the sample under investigation. The filled squares represent the experimental data, while the lines show the best fit to them.

laser intensities. The scatter of the experimental data with respect to the fit in this figure is naturally larger than that of the original data due to the differentiation. Nevertheless, the values for the radiative lifetime τ_r and the nonradiative lifetimes τ_{nr} are essentially identical for both fits. We obtain $\tau_r = (80\pm24)$ ns and $\tau_{nr} = (19\pm3)$ ns. (The error bars represent the statistical confidence levels for the fit to the original data.) This surprisingly short radiative lifetime corresponds to a background hole density of $p_0 = 10^{10}$ cm^{-2}, rather high for an intentionally undoped quantum well grown by MBE. For comparison, the minimum (maximum) laser intensity of 1.2 W/cm^2 (660 W/cm^2) creates an excess carrier density of 7.4×10^8 cm^{-2} (1.3×10^{11} cm^{-2}) as determined by the steady-state solution for Δn of Eq. (4). (Note that the carrier density is proportional to the square root of the laser intensity for large-signal excitation.) The previously defined constant G^* [Eq. (6)] obtained from the fit corresponds to a laser intensity of 40 W/cm^2 and a carrier density of 2×10^{10} cm^{-2}, above which the radiative recombination dominates over the nonradiative one. We stress that the accuracy of all these values, particularly for the radiative and nonradiative lifetimes, depends on the numerical values assumed for the radiative recombination coefficient B and the absorption probability per layer p. As we will see in Sec. III C, our estimate of these two quantities seems to be quite accurate, as the actual lifetimes directly measured under transient conditions are in excellent agreement with the above-derived values.

B. Transient conditions

Transient PL measurements are performed at 300 K using a dye laser as the excitation source, which is synchronously pumed by a mode-locked N_2 laser with a repetition rate of 10 Hz. The pulse width is ≤ 1 ns at an excitation wavelength of 644 nm. The PL decay is measured for a range of incident fluences, adjusted by neutral density filters, up to the maximum available fluence of 80 μJ cm^{-2}. The emitted light is detected by a synchroscan streak camera following a 25-cm spectrometer.

Figure 6 presents examples for the PL decay of the sample under investigation after pulsed excitation with a fluence of 80 μJ cm^{-2}. The solid line represents the fit of Eq. (7) to the experimental data. Excitonic effects are included using the values for σ_x and b_x given in Sec. III A. Such complete fits are slightly, but not substantially, better than those obtained if excitons are neglected. In any case, the fits give unique values for the radiative and nonradiative lifetimes which do not depend on the injection level. The average over all measurements yields $\tau_r = (91\pm40)$ ns and $\tau_{nr} = (17.5\pm7)$ ns. These values are in very satisfactory agreement with those derived from the steady-state measurements presented above, which demonstrates the consistency of our model. Furthermore, we obtain the actual initial carrier densities for each of the measurements whose ratio is in good agreement with the one expected from the experimental conditions. For the maximum fluence, we obtain $\Delta n_0 = 1\times10^{11}$ cm^{-2}, which is still below the onset of exciton screening.[24]

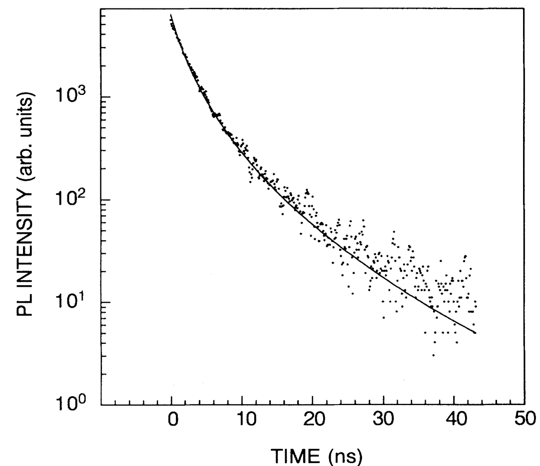

FIG. 6. Transient PL intensity of the sample under investigation after pulsed excitation with a fluence of 80 μJ cm^{-2}. The filled circles represent experimental data, while the lines show the best fit to them.

The values derived for the radiative and nonradiative lifetimes for the present sample are quite remarkable indeed. Evidently, the radiative lifetime is rather short, and suggests a background doping 1–2 orders of magnitude higher than typical values for MBE-grown material. Furthermore, the nonradiative lifetime is extraordinarily long in comparison to literature values. Recent measurements of the nonradiative lifetime in (100)-oriented $In_{0.1}Ga_{0.9}As/Al_{0.2}Ga_{0.8}As$ multiple quantum wells gave values around 500 ps.[25] The reason for these interesting features of our sample has not yet been clarified beyond doubt, but it seems very likely to originate from the specific bonding configuration of the (311)A surface. In fact, the single dangling bonds present on the (311)A surface are believed to substantially reduce the incorporation of deep-level impurities,[26] particularly oxygen.[27] Oxygen tends to accumulate at the inverted interface of QW's with $Al_xGa_{1-x}As$ barriers, and is the most likely candidate for the dominating nonradiative defect in such structures.[27] In any case, a lower density of interface recombination centers would, of course, reduce the nonradiative recombination rate, and, additionally, result in a lower degree of compensation of shallow acceptors (for which the deep-level impurities act as traps) and thus a higher background hole density.[28] A detailed account of these material aspects will be published in a forthcoming paper.

IV. SUMMARY AND CONCLUSIONS

The model developed in this work describes the recombination dynamics in quantum wells under both steady-state and transient conditions, considering the coexistence of excitons, free carriers, and nonradiative recombination centers. We have derived explicit expressions for the photoluminescence intensity as a function of generation rate and of time, and, in each case, have discussed the influence of the various recombination channels on the respective behavior of the PL intensity. For steady-

state conditions, excitons and free carriers cannot be distinguished from each other. For transient conditions, excitons may be neglected only for the special case of undoped GaAs-based QW's at RT, while their inclusion becomes important in lightly doped material, for lower temperature ($\simeq 77$ K), and for materials with a substantially larger ($4\times$) exciton binding energy such as, e.g., II-VI compounds. Nonradiative recombination substantially modifies the recombination dynamics under both steady-state and transient conditions and must not, therefore, be neglected *a priori.* Despite the simplicity of our model, the predicted dependences of the PL intensity on generation rate and time are, in general, complex, and are not as straightforwardly interpretable as previously believed. For a reliable identification of the participating recombination channels it is of great advantage to perform measurements under both steady-state and transient conditions over the largest dynamic range technically feasible. For a practical demonstration, we fitted the theoretical expressions for the PL intensity to such a set of experimental data, taken at 300 K from a high quality single $In_{0.1}Ga_{0.9}As/Al_{0.33}Ga_{0.67}As$ quantum well. The consistency of our model is demonstrated by the good agreement of the small-signal radiative and nonradiative lifetimes derived from the fits for steady-state and transient conditions. Though the sample investigated exhibits an extraordinarily long nonradiative lifetime, the PL decay is still largely controlled by the nonradiative process. Thus the consideration of nonradiative recombination is, in general, of vital importance given the fact that it remains of significant magnitude even in present state-of-the-art samples.

ACKNOWLEDGMENTS

We are indebted to Mari Tsugami at the Optoelectronic and Microwave Devices Laboratory of Mitsubishi Electric Corporation for her cooperation concerning the time-resolved photoluminescence measurements. Furthermore, we thank Bryan Banish and Anno Hermanns for critical readings of the manuscript.

---

*Permanent address: Paul-Drude-Institut für Festkörperelektronik, Hausvogteiplatz 5-7, D-10117 Berlin, Germany.

[1] For an excellent introduction to recombination processes see, e.g., P. T. Landsberg, in *Handbook on Semiconductors,* edited by T. S. Moss (North-Holland, Amsterdam, 1982), Vol. 2. A comprehensive overview of radiative recombination (photoluminescence) is given in the classical text of H. B. Bebb and E. W. Williams, in *Semiconductors and Semimetals,* edited by R. K. Willardson and A. C. Beer (Academic, London, 1972), Vol. 8.

[2] W. Pickin and J. P. R. David, Appl. Phys. Lett. **56**, 268 (1990).

[3] B. K. Ridley and P. J. Bishop, IEEE Proc. J. **138**, 294 (1991).

[4] For models describing the steady-state recombination dynamics for cases where impurity and bound-exciton transitions are important, see L. E. Oliveira and M. de Dios-Leyva, Phys. Rev. B **48**, 15 092 (1993); T. Schmidt, R. Lischka, and W. Zulehner, *ibid.* **45**, 8989 (1992).

[5] D. Bimberg, J. Christen, A. Werner, M. Kunst, G. Weimann, and W. Schlapp, Appl. Phys. Lett. **49**, 76 (1986); P. J. Bishop, M. E. Daniels, B. K. Ridley, and K. Woodbridge, Phys. Rev. B **45**, 6686 (1992).

[6] J. Christen and D. Bimberg, Phys. Rev. B **42**, 7213 (1990); M. Colocci, M. Gurioli, and A. Vinattieri, J. Appl. Phys. **68**, 2809 (1990).

[7] P. Dawson, G. Duggan, H. I. Ralph, and K. Woodbridge, Phys. Rev. B **28**, 7381 (1983); K. Fujiwara, N. Tsukada, and T. Nakayama, Appl. Phys. Lett. **53**, 675 (1988).

[8] J. E. Fouquet and A. E. Siegman, Appl. Phys. Lett. **46**, 280 (1985); K. Fujiwara, A. Nakamura, Y. Tokuda, T. Nakayama, and M. Hirai, *ibid.* **49**, 1193 (1986); B. Sermage, F. Alexandre, J. Beerens, and P. Tronc, Superlatt. Microstruct. **6**, 373 (1989); M. Gurioli, A. Vinattieri, M. Colocci, A. Bosacchi, and S. Franchi, Appl. Phys. Lett. **59**, 2150 (1991).

[9] B. K. Ridley, Phys. Rev. B **41**, 12 190 (1990).

[10] Here we neglect, for simplicity, terms describing the thermal ionization of recombination centers which are, in principle, necessary to guarantee that the total rate vanishes at equilibrium. For the present discussion these terms are not important.

[11] R. K. Ahrenkiel, B. M. Keyes, and D. J. Dunlavy, J. Appl. Phys. **70**, 225 (1991).

[12] D. C. Martin, S. C. Moss, and L. F. Halle, J. Appl. Phys. **72**, 1970 (1992).

[13] J. Singh, in *Solid State Physics,* edited by H. Ehrenreich and D. Turnbull (Academic, Orlando, FL, 1984), Vol. 38.

[14] E. H. Böttcher, K. Ketterer, D. Bimberg, G. Weimann, and W. Schlapp, Appl. Phys. Lett. **50**, 1074 (1987).

[15] Y. J. Ding, C. L. Guo, J. B. Khurgin, K.-K. Law, and J. L. Merz, Appl. Phys. Lett. **60**, 2051 (1992).

[16] E. Yablonovitch, T. J. Gmitter, and R. Bhat, Phys. Rev. Lett. **61**, 2546 (1988).

[17] The absorption probability per layer is given by

$$p=\frac{\pi e^2}{\hbar m_0^2\omega c_0\epsilon_0}\frac{2|p_{cv}|^2}{1+e^{-2\gamma}}\frac{\mu}{\pi\hbar^2}\Theta(\hbar\omega-E_G)\ ,$$
$$\gamma=\pi\sqrt{E_x/(\hbar\omega-E_G)}\ ,$$

where we have assumed, as above, that excitation is not resonant to the exciton state but takes place in the continuum above the subband gap E_G. For the present parameters we obtain $p=0.0125$, i.e., each quantum well absorbs, almost independently of its well width, about 1% of the incident light. This formulation avoids ambiguities related to the definition of an absorption coefficient per unit length [see, e.g., O. Brandt, H. Lage, and K. Ploog, Phys. Rev. B **43**, 14 285 (1991), and references therein].

[18] J. Christen and D. Bimberg, Surf. Sci. **174**, 261 (1986).

[19] Y. Arakawa, H. Sakaki, M. Nishioka, J. Yoshino, and T. Kamiya, Appl. Phys. Lett. **46**, 519 (1985).

[20] L. C. Andreani, F. Tassone, and F. Bassani, Solid State Commun. **77**, 641 (1991).

[21] D. S. Citrin, Phys. Rev. B **47**, 3832 (1993).

[22] In the usual three-dimensional formulation (which is, generally, to be avoided since it introduces a spurious explicit well-width dependence), these values correspond to $b_rL_z=3.6\times10^{-10}$ cm^3/s and $b_xL_z=2.4\times10^{-10}$ cm^3/s, respectively, where L_z is the well width. Actually, b_r is implicitly dependent on well width via the overlap integral, whereas b_x exhib-

its a stronger implicit well-width dependence via the oscillator strength.

[23]M. T. Emeny, M. S. Skolnick, C. R. Whitehouse, D. G. Hayes, P. D. J. Calcott, and A. W. Higgs, Appl. Phys. Lett. **63**, 824 (1993), and references therein.

[24]Note that this carrier concentration is substantially lower than that expected if assuming unity capture efficiency for carriers created in the barrier. In fact, strong luminescence is observed from both the barriers and the buffer superlattice.

[25]M. H. Moloney, J. Hegarty, L. Buydens, P. Demeester, R. Grey, and J. Woodhead, Appl. Phys. Lett. **62**, 3327 (1993).

[26]I. W. Tao, C. Schwartz, and W. I. Wang, J. Vac. Sci. Technol. B **10**, 838 (1992).

[27]N. Chand, Thin Solid Films **231**, 143 (1993).

[28]R. Zucca, J. Appl. Phys. **48**, 1987 (1977); M. S. Gorsky, T. F. Kuech, F. Cardone, P. M. Mooney, G. J. Scilla, R. M. Mooney, G. J. Scilla, and R. M. Potemski, Appl. Phys. Lett. **58**, 1979 (1991).